

## All in-situ study on topological insulator heterostructures

*Simone G. Altendorf<sup>#</sup>, Christoph Becker, Chun-Fu Chang, Arnold Choa, Katharina Höfer, Cariad-A. Knight, Alexander C. Komarek, Cevriye Koz, Chang-Yang Kuo, Sheng-Chieh Liao, Cheng-En Liu, Vanda M. Pereira, A. Diana Rata, Sahana Rößler, Ulrich Schwarz, Jesse Swanson, Liu Hao Tjeng, Steffen Wirth, Chi-Nan Wu*

**Heterostructures have been in the focus of the recent topological insulator research since they show a variety of spectacular novel phenomena and allow for a precise tailoring of the electronic band structure. In our advanced ultra-high vacuum system, we prepared bulk insulating thin films of the topological insulator  $\text{Bi}_2\text{Te}_3$  by molecular beam epitaxy and interfaced them with magnetic oxides and the topological insulator  $\text{Sb}_2\text{Te}_3$ . The characterization was performed in-situ or protected by Tellurium capping to avoid uncontrolled doping due to exposure to air causing topologically trivial conduction. Our results indicate a gap opening at the surface states for the magnetic heterostructures and show how the surface states and the band structure are modulated when interfacing two topological insulators with complementary electronic character. Moreover, we studied the growth of FeTe films - a potential candidate for superconductor / topological insulator interfaces.**

Topological insulator (TI) heterostructures have been shown to offer a large playground to study and manipulate topological surface states. By interfacing TIs with magnets or superconductors, for example, exotic phenomena such as the quantum anomalous Hall effect (QAHE) or Majorana states can be induced.

The experimental research on TIs, however, carries an inherent issue namely the typically small number of topologically relevant charge carriers ( $\sim \text{few } 10^{12}\text{cm}^{-2}$ ). The exciting TI properties are easily masked or even overwhelmed by topologically trivial conduction due to defects in the bulk or at the surface. From the band structure, one can estimate that an extremely high purity of the materials with less than 1% surface defects and a bulk defect concentration of well below parts per million level is required. Thus, it is not surprising that the experimental realization of the theoretical predicted phenomena is often hindered by an insufficient sample quality. This stresses the need of extremely high-quality bulk-insulating materials with ultra-clean surfaces and interfaces which can be only achieved using sophisticated sample preparations and taking special precautions during the measurements.

Our state-of-art in-house ultra-high vacuum system allows for the growth and in-situ characterization of high-quality topological insulator thin films and heterostructures. In our previous studies [1, 2], we have successfully optimized the molecular beam epitaxy (MBE) growth conditions for the preparation of  $\text{Bi}_2\text{Te}_3$  topological insulator thin films on  $\text{Al}_2\text{O}_3$  and  $\text{BaF}_2$  substrates that show truly bulk insulating behavior with only the characteristic Dirac-like surface states intersecting the Fermi level. Moreover, we have established a routine for the sample characterization under cleanest conditions by in-situ reflection high-

energy electron diffraction (RHEED), low energy electron diffraction (LEED), x-ray photoelectron spectroscopy (XPS), angle-resolved photoelectron spectroscopy (ARPES), and temperature-dependent resistivity measurements, and developed a reliable capping procedure with crystalline Tellurium for complementary ex-situ measurements. An overview on the challenging work on topological insulator thin films is also given in our review paper [3]. The focus of our recent work is now to investigate the influence of interfacing  $\text{Bi}_2\text{Te}_3$  with the magnetic insulators  $\text{Fe}_3\text{O}_4$ ,  $\text{Y}_3\text{Fe}_5\text{O}_{12}$ , and  $\text{Tm}_3\text{Fe}_5\text{O}_{12}$ , as well as with the topological insulator  $\text{Sb}_2\text{Te}_3$ . We also optimize the growth and composition of FeTe thin films, which build - in proximity to Te-based TIs like  $\text{Bi}_2\text{Te}_3$  - a promising platform to study the physics of superconductor / TI heterostructures.

### 1. Interfacing $\text{Bi}_2\text{Te}_3$ with magnetic oxides [3, 4, 5]

Introducing magnetic order in TI systems breaks the time reversal symmetry which can induce an opening of a gap at the TI surface states and thus, can cause novel phenomena such as the QAHE. Magnetic ordering can be experimentally achieved by doping the TI with magnetic ions or by utilizing the magnetic proximity effect at the interface with magnetic materials. We pursue the latter approach which has the advantage of a significantly larger temperature window for the observation of the induced effects due to a higher Curie temperature of the magnetic layer and a more uniform magnetization at the interface. Furthermore, the choice of magnetic insulator materials over e.g. magnetic metals reduces the risk of strong chemical reactions at the interface or current shunting through the magnetic layer.

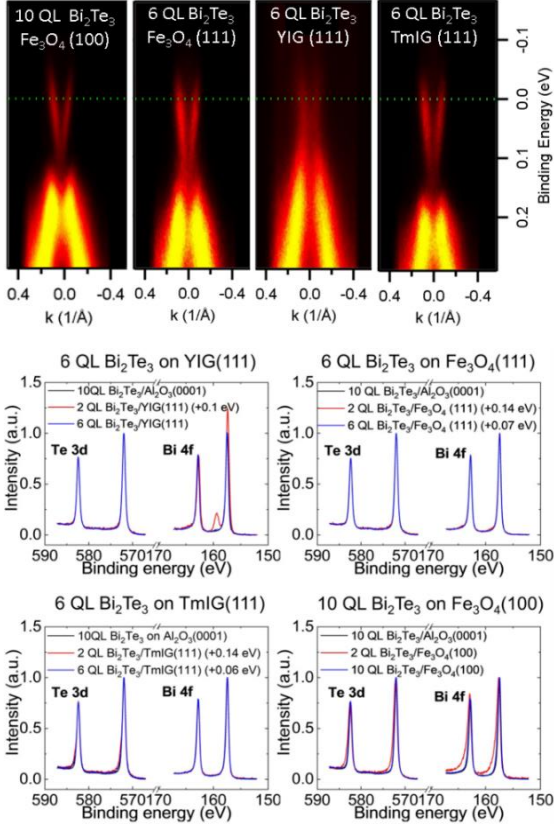


Fig. 1: ARPES (top) and XPS (bottom) measurements of 6-10 QL  $\text{Bi}_2\text{Te}_3$  on  $\text{Fe}_3\text{O}_4$  (100),  $\text{Fe}_3\text{O}_4$  (111), YIG (111), TmIG (111). [3, 5]

### 1.1 Growth of $\text{Bi}_2\text{Te}_3$ on $\text{Fe}_3\text{O}_4$ , YIG, and TmIG

As magnetic layers, we chose  $\text{Fe}_3\text{O}_4$  (001) films,  $\text{Fe}_3\text{O}_4$  (111) crystals,  $\text{Y}_3\text{Fe}_5\text{O}_{12}$  (YIG) (111) crystals, and  $\text{Tm}_3\text{Fe}_5\text{O}_{12}$  (TmIG) (111) films because of their well-established growth procedures, high Curie temperatures, or known compatibility with TIs. To avoid chemical reactions between  $\text{Bi}_2\text{Te}_3$  and the magnetic oxides, the MBE growth conditions established for  $\text{Bi}_2\text{Te}_3$  on  $\text{Al}_2\text{O}_3$  and  $\text{BaF}_2$  substrates were adapted. The first two quintuple layers (QLs) were grown at room temperature (instead of 160-185°C) followed by an annealing at 240°C to crystallize the deposited layer. In a second step, the  $\text{Bi}_2\text{Te}_3$  layers were grown at 220°C to the desired thickness.

As indicated by the ARPES spectra in Fig. 1 (top), all films grown in these conditions have an insulating bulk with defined surface states crossing the Fermi level, similar to the  $\text{Bi}_2\text{Te}_3$  films grown on the nonmagnetic  $\text{Al}_2\text{O}_3$  and  $\text{BaF}_2$  substrates. XPS measurements of 2 and 6(10) QL  $\text{Bi}_2\text{Te}_3$  for the various substrates are shown in Fig. 1 (bottom). The Te 3d and Bi 4f core level spectra of the very thin layers indicate that there are no significant chemical reactions at the interface. Only the

film grown on  $\text{Fe}_3\text{O}_4$  (100) shows small shoulders at higher binding energies of the Te and Bi core levels indicating some Te-O and Bi-O bonds, however, no formation of Te or Bi oxides is observed. For the thicker layers, the spectra are identical to the films grown on  $\text{Al}_2\text{O}_3$  and  $\text{BaF}_2$ . It is thus expected that the magnetic proximity effect is present for all these  $\text{Bi}_2\text{Te}_3$  / magnetic oxide heterostructures.

### 1.2 Transport and x-ray magnetic circular dichroism studies of $\text{Bi}_2\text{Te}_3$ on magnetite and iron garnets

The influence of the proximity of the magnetic layers on the TI was further investigated by transport measurements. The magnetoconductance curves in Fig. 2(a) show a cusp-like behavior for the reference sample grown on nonmagnetic  $\text{Al}_2\text{O}_3$  revealing the weak antilocalization effect typical for TIs, while a flattening of the curves is observed for the films grown on the magnetic substrates. This deviation suggests a suppression of the weak antilocalization effect and an induction of the weak localization effect which is in agreement with a formation of a gap at the topological surface states.

Furthermore, the Hall resistance measurements (Figs. 2(b-c)) show the occurrence of the anomalous Hall effect (AHE) for 6 QLs of  $\text{Bi}_2\text{Te}_3$  grown on YIG (111), TmIG (111), and  $\text{Fe}_3\text{O}_4$  (111) supporting the presence of interfacial magnetism. Only for the TI grown on  $\text{Fe}_3\text{O}_4$  (100), no AHE was observed which might be related to the dead magnetic layer typically formed at this magnetite surface.

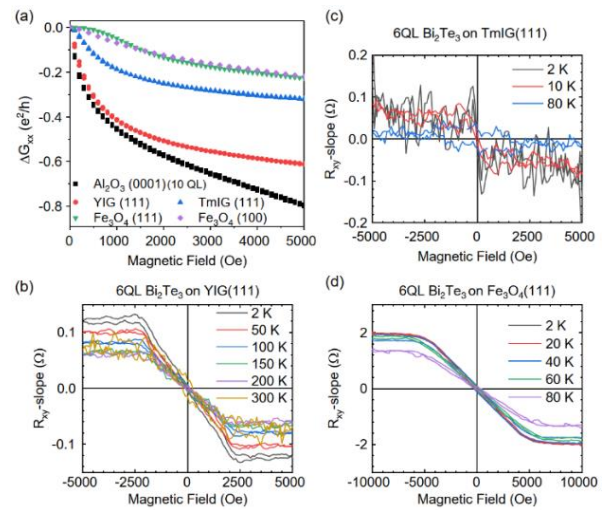


Fig. 2: (a) Magnetoconductance at 2 K for 6 QL  $\text{Bi}_2\text{Te}_3$  grown on YIG (111), TmIG (111),  $\text{Fe}_3\text{O}_4$  (111),  $\text{Fe}_3\text{O}_4$  (100), as well as a reference 10 QL  $\text{Bi}_2\text{Te}_3$  film on  $\text{Al}_2\text{O}_3$  (0001). (b-c) Hall resistances. A linear background (the ordinary Hall effect) was subtracted to emphasize the anomalous Hall effect. [3]

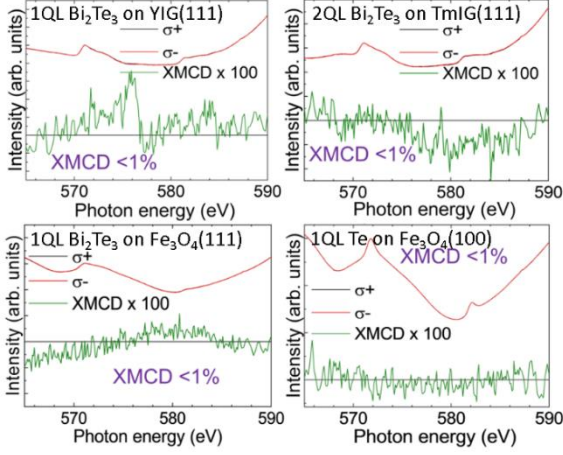


Fig. 3: X-ray absorption and XMCD spectra of the Te  $M_{4,5}$  edges of Te and  $\text{Bi}_2\text{Te}_3$  films deposited on the magnetic insulators. [5]

To study the origin of the AHE in more detail, in-situ x-ray magnetic circular dichroism (XMCD) measurements were performed at the NSRRC in Taiwan. While the Fe  $L_{2,3}$  absorption edges clearly show a strong XMCD signal for all substrates confirming their magnetic character, the Te  $M_{4,5}$  edges of ultra-thin Te and  $\text{Bi}_2\text{Te}_3$  films deposited on the magnetic insulators do not show any detectable XMCD ( $<1\%$ ) (Fig. 3). The observation of no XMCD at the Te edges, while weak localization and AHE hint towards a proximity induced magnetization, is at the first sight surprising but it can be understood by considering the size of the exchange gap which is in the order of only 10 meV. A rough estimate of the XMCD effect can be obtained by subtracting two Te  $M_{4,5}$  absorption spectra which are shifted by  $\pm E_{\text{gap}}/2$  resulting in an XMCD of only 1.6%. In addition, one should keep in mind that due to the weak Van-der-Waals forces only a very thin layer of the  $\text{Bi}_2\text{Te}_3$  film close to the magnetic substrate is magnetized and contributes to the XMCD effect. Considering that only 1 monolayer of 1 QL  $\text{Bi}_2\text{Te}_3$  is actually magnetized, then the XMCD effect decreases to 0.3%, well below the detection limit. This result also

shows that an observation of a strong XMCD signal at the Te  $M_{4,5}$  edges of such heterostructures can be an indication for significant intermixing at the interface.

## 2. Freeing of the Dirac point in $\text{Sb}_2\text{Te}_3/\text{Bi}_2\text{Te}_3$ heterostructures [6]

Interfacing different TI materials can also lead to significant modifications of the TI properties. Such TI/TI heterostructures are of great interest since they allow for an engineering of the band structure. To have direct access to the TI properties by transport measurements – to observe for example the QAHE, the materials should ideally have a highly insulating bulk and an exposed Dirac point at or close to the Fermi level – characteristics that most TIs unfortunately do not have naturally. A combination of TI materials with complementary electronic properties in ternary (or quaternary) compounds or in heterostructures has been shown to be a successful approach to tailor the band structure to come closer to an ideal TI.

We systematically study the evolution of the band structure of  $\text{Sb}_2\text{Te}_3/\text{Bi}_2\text{Te}_3$  heterostructures from very thin (1 QL) to very thick (40 QLs)  $\text{Sb}_2\text{Te}_3$  adlayers using in-situ ARPES. Figure 4 (left) shows the ARPES spectra close to the Fermi level ( $E_F$ ) for various adlayer thicknesses. The Dirac point shifts considerably, by  $\sim 240$  meV, from below the Fermi level to above, crossing it for an adlayer thickness of about 10 QLs. In Fig. 4 (right), the energy distribution curves of the spectra integrated around  $k=0$  are shown. Here the characteristics of the bulk structure become evident revealing that also the bulk features undergo significant changes. For a better understanding of the evolution, which is essential for a controlled engineering of the band structure, it is thus important to distinguish the different contributions, namely the shift of the surface states, the shift of the bulk states, and the shift of the entire band structure due to a change of the chemical potential.

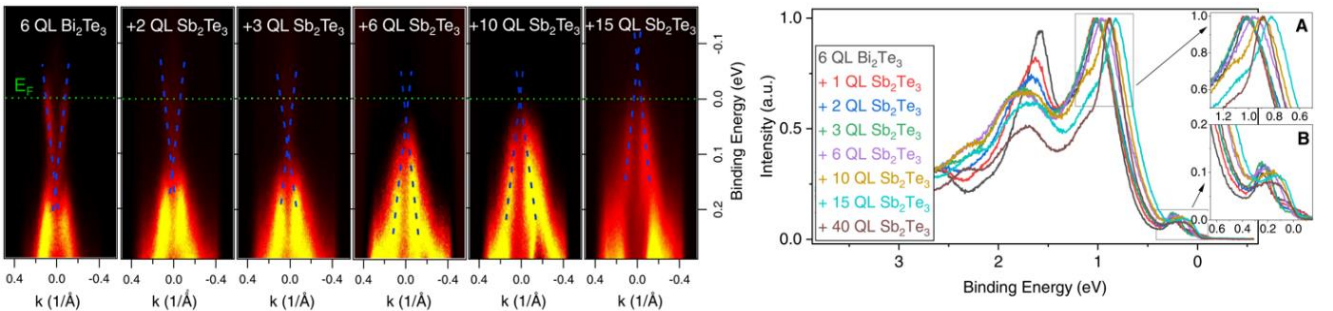


Fig. 4: Electronic structure of 0-40 QL  $\text{Sb}_2\text{Te}_3$  on 6 QL  $\text{Bi}_2\text{Te}_3$ . Left: ARPES spectra measured along the  $\Gamma$ -K direction. The topological surface states are indicated by the dashed blue lines. Right: Energy distribution curves integrated around  $k=0$  showing the evolution of the bulk features. [6]

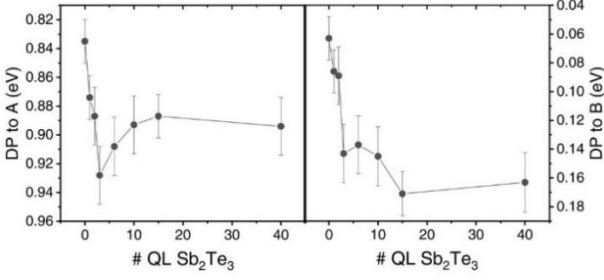


Fig. 5: Position of the Dirac point in relation to bulk features **A** (left) and **B** (right). [6]

First, the bulk behavior is characterized for the different adlayer thicknesses by tracking the two common bulk features **A** (at  $\sim 1.0$  eV binding energy) and **B** (at  $\sim 0.2$  eV), see insets in Fig. 4. The positions of **A** and **B** relative to the Fermi level are rather constant for 0-3 QLs of  $\text{Sb}_2\text{Te}_3$  and shift considerably for the larger thicknesses, showing a trend similar to the surface states in relation to the Fermi level. This indicates that for the larger thicknesses the entire band structure shifts due to a shift of the chemical potential. Moreover, a change in the distance of bulk features **A** and **B** is observed. Tracking the relative positions of **A** and **B**, a gradual decrease of the separation by about 60 meV is observed for adlayers with thicknesses in the range of 4-10 QLs. This reveals a gradual change from  $\text{Bi}_2\text{Te}_3$  to  $\text{Sb}_2\text{Te}_3$  bulk character for these intermediate thicknesses.

Having established the evolution of the bulk features, one can now plot the position of the Dirac point in relation to bulk features **A** and **B** (Fig. 5), thereby excluding contributions from chemical potential shifts. One can clearly see that the important modulation of the surface states happens very rapidly for the first

3 QLs of  $\text{Sb}_2\text{Te}_3$ . For larger thicknesses, the values are rather constant indicating that surface and bulk states are moving rigidly together. Thus, the band structure engineering in  $\text{Sb}_2\text{Te}_3/\text{Bi}_2\text{Te}_3$  can be summarized as follows: The very first adlayers are essential for a freeing of the Dirac point from the valence band into the bulk band gap, while the shift of the chemical potential for the thicker adlayers allows for an alignment of the Dirac point with the Fermi level.

### 3. $\text{Fe}_{1+y}\text{Te}$ thin films – a potential material for superconductor / TI heterostructures [7]

$\text{FeTe}$  is a parent compound of the Fe-based superconductors. Surprisingly the material itself is, in contrast to  $\text{FeSe}$ , not superconducting which might be related to the excess of Fe that is typically incorporated in the  $\text{Fe}_{1+y}\text{Te}$  structure, see also [https://www1.cpfs.mpg.de/2443/COLL\\_01](https://www1.cpfs.mpg.de/2443/COLL_01). Recent studies report on the occurrence of superconductivity at the interface of  $\text{FeTe}$  and  $\text{Bi}_2\text{Te}_3$  or  $\text{Sb}_2\text{Te}_3$  which is speculated to be induced by a charge transfer causing a weakening of the antiferromagnetic order.

The objective of our work is to control the excess of Fe in  $\text{Fe}_{1+y}\text{Te}$  films using Te-limited conditions in the MBE growth process, thereby coming closer to the stoichiometric, possibly superconducting composition which would be a promising starting material for a more detailed study on the interface effects in proximity to Te-based TIs. X-ray absorption and XMCD measurements were performed to study the electronic structure as well as the magnetic character of  $\text{Fe}_{1+y}\text{Te}$  films grown at various Te fluxes keeping the Fe flux constant, see exemplary results in Fig. 6. The

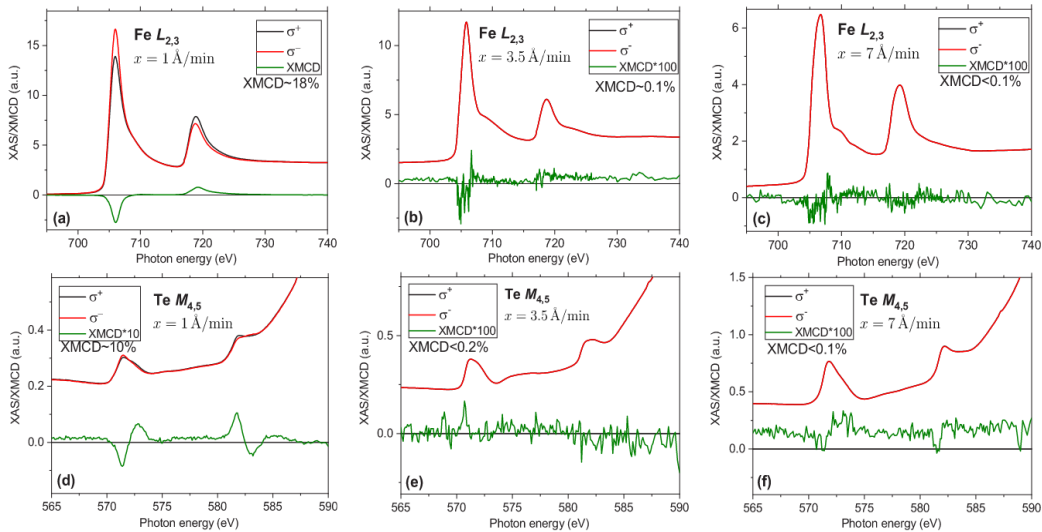


Fig. 6:  $\text{Fe } L_{2,3}$  and  $\text{Te } M_{4,5}$  XAS and XMCD spectra for  $\text{Fe}_{1+y}\text{Te}$  thin films grown with Te flux rate  $x=1\text{Å}/\text{min}$  (a,d),  $x=3.5\text{Å}/\text{min}$  (b,e), and  $x=7\text{Å}/\text{min}$  (c,f). The Fe flux rate is set to  $1\text{Å}/\text{min}$  for all films. [7]

XMCD effect at the Fe  $L_{2,3}$  and Te  $M_{4,5}$  edges for the low Te rates of 1-2 Å/min indicate a formation of presumably Fe metal clusters that are ferromagnetically ordered. These magnetic clusters are not present for the higher Te fluxes as indicated by the absence of any detectable XMCD signal. For Te rates of 2.5–3.5 Å/min, RHEED reveals a layer-by-layer growth of  $\text{Fe}_{1+y}\text{Te}$  films with a composition ranging from  $\text{Fe}_{1.60}\text{Te}$  to  $\text{Fe}_{1.14}\text{Te}$ , in which the excess Fe resides interstitially. For a Te rate of 4 Å/min, we may have achieved the stoichiometric  $\text{Fe}_{1.00}\text{Te}$  compound and, for higher Te rates,  $\text{FeTe}_2$  starts to form, as indicated by x-ray absorption and x-ray diffraction measurements. Thus, our new preparation route allows to grow  $\text{Fe}_{1+y}\text{Te}$  films with a much wider composition range than reported for bulk single crystals and may indeed provide an opportunity to synthesize superconducting FeTe.

#### 4. Conclusions

Heterostructures of  $\text{Bi}_2\text{Te}_3$  interfaced with magnetic oxides and  $\text{Sb}_2\text{Te}_3$  were systematically studied to investigate changes in the transport properties and in the band structure. We carefully avoid contributions of topologically trivial conduction from defects by thorough optimization of growth conditions and in particular of the interface. Furthermore, any degradation of the surface under ambient conditions is circumvented by a preparation and characterization all under ultra-high vacuum conditions, or if unavoidable by capping with crystalline Tellurium. For the magnetic heterostructures, the occurrence of the anomalous Hall effect and the suppression of the weak antilocalization effect indicate an opening of the gap at the surface states induced by the magnetic proximity effect. X-ray absorption measurements, however, show no XMCD signal on the Te edges. This suggests that the magnetism induced by the weak Van-der-Waals coupling is too small to be detected by XMCD but still can be seen in the transport measurements. For the  $\text{Sb}_2\text{Te}_3/\text{Bi}_2\text{Te}_3$  heterostructures, we were able to differentiate the contributions to the changes in the band structure. Our results point out the crucial role of the very first adlayers for the freeing of the Dirac point in  $\text{Bi}_2\text{Te}_3$ . This yields important insights for the design of TI heterostructures with tailored properties.

Moreover, we developed a new MBE growth procedure for the preparation of  $\text{Fe}_{1+y}\text{Te}$  films using Te-limited conditions which allows for the synthesis of a very wide range, much larger compared to the bulk crystals, of Fe contents. Our results indicate that it might be possible to grow close to stoichiometric FeTe

in thin film form which might have superconducting character and is thus a promising candidate to investigate  $\text{Bi}_2\text{Te}_3$  / superconductor heterostructures.

#### External Cooperation Partners

M. Guo, J. Kwo (National Tsing Hua University, Hsinchu, Taiwan); M. Hong (National Taiwan University, Taipei, Taiwan); H.-J. Lin, C. T. Chen (NSRRC, Hsinchu, Taiwan).

#### References

- [1] *Intrinsic conduction through topological surface states of insulating  $\text{Bi}_2\text{Te}_3$  epitaxial thin films*, K. Höfer, C. Becker, A. D. Rata, J. Swanson, P. Thalmeier, and L. H. Tjeng, *Proc. Natl. Acad. Sci. U.S.A.* **III** (2014) 14979.
- [2] *Protective capping of topological surface states of intrinsically insulating  $\text{Bi}_2\text{Te}_3$* , K. Höfer, C. Becker, S. Wirth, and L. H. Tjeng, *AIP Advances* **5** (2015) 097139.
- [3]\* *Challenges of Topological Insulator Research:  $\text{Bi}_2\text{Te}_3$  Thin Films and Magnetic Heterostructures*, V. M. Pereira, C.-N. Wu, K. Höfer, A. Choa, C.-A. Knight, J. Swanson, C. Becker, A. C. Komarek, A. D. Rata, S. Rößler, et al., *Phys. Status Solidi B* **258** (2021) 2000346.
- [4]\* *Interfacing topological insulators and ferrimagnets:  $\text{Bi}_2\text{Te}_3$  and  $\text{Fe}_3\text{O}_4$  heterostructures grown by molecular beam epitaxy*, V. M. Pereira, C. N. Wu, C.-A. Knight, A. Choa, L. H. Tjeng, and S. G. Altendorf, *APL Mater.* **8** (2020) 071114.
- [5]\* *Topological insulator interfaced with ferromagnetic insulators:  $\text{Bi}_2\text{Te}_3$  thin films on magnetite and iron garnets*, V. M. Pereira, S. G. Altendorf, C. E. Liu, S. C. Liao, A. C. Komarek, M. Guo, H.-J. Lin, C. T. Chen, M. Hong, J. Kwo, L. H. Tjeng, and C. N. Wu., *Phys. Rev. Mater.* **4** (2020) 064202.
- [6]\* *Modulation of surface states in  $\text{Sb}_2\text{Te}_3/\text{Bi}_2\text{Te}_3$  topological insulator heterostructures: The crucial role of the first adlayers*, V. M. Pereira, C. N. Wu, L. H. Tjeng, and S. G. Altendorf, *Phys. Rev. Mater.* **5** (2021) 034201.
- [7]\* *Molecular beam epitaxy preparation and in situ characterization of FeTe thin films*, V. M. Pereira, C. N. Wu, C. E. Liu, S.-C. Liao, C. F. Chang, C.-Y. Kuo, C. Koz, U. Schwarz, H.-J. Lin, C. T. Chen, L. H. Tjeng, and S. G. Altendorf, *Phys. Rev. Mater.* **4** (2020) 023405.

# Simone.Altendorf@cpfs.mpg.de